LBL-11770
Preprint

Lawrence Berkeley Laboratory
UNIVERSITY OF CALIFORNIA

Physics, Computer Science &
Mathematics Division

Submitted for publication

TOPOLOGICAL THEORY OF HADRONS II: BARYONS

Henry P. Stapp

October 1981

Prepared for the U.S. Department of Energy under Contract W-7405-ENG-48

DISCLAIMER

TOPOLOGICAL THEORY OF HADRONS II: BARYONS

Henry P. Stapp

Lawrence Berkeley Laboratory
University of California
Berkeley, California 94720

ABSTRACT

The first paper of this series described a method for incorporating spin into the meson sector of the topological theory of hadrons. This second paper extends the theory to all hadrons. It also incorporates into the covariant S-matrix topological framework the group-theoretic properties of the constituent quark model.

* This work was supported by the Director, Office of Energy Research, Office of High Energy and Nuclear Physics, Division of High Energy Physics of the U.S. Department of Energy under Contract W-7405-ENG-48.

1. EARLY ATTEMPTS

The early attempts [1-6] to include baryons in the topological expansion corresponded to picturing the baryon as a set of three surfaces arranged like the feathers of an arrow, with each outer edge a quark line and all three inner edges placed in close proximity to a single "dotted" line called by various authors a dotted, junction, or mating line. Within the context of the topological expansion this picture arose in several ways, first as the basis of a simple solution to the purely topological problem of extending the meson topological expansion scheme to three-quark baryons [1], then from ideas based on QCD [2,3], and finally from attempts to extend to baryons the idea of the ordered S-matrix [4,5]. These different approaches all led to essentially the same conclusion regarding the nature of surfaces of zero complexity, or zero entropy: the zero-entropy surfaces were those that could be generated from a disc by a finite number of operations, each of which consists of attaching two new discs to some linear portion of the boundary of the surface obtained from the proceeding operations, as indicated in Fig. 1.

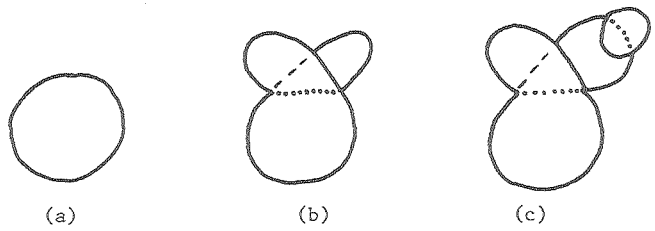

Figure 1

Three Elementary surfaces

The surfaces that can be constructed by this procedure are called elementary surfaces [6].

One defect of this identification of zero-entropy surfaces with elementary surfaces arises from the fact that an elementary surface is separated by a cut into two elementary surfaces if and only if the cut is a tree graph [6]. Thus if a non-tree-graph cut separates an elementary surface into two connected parts then these two parts are not both elementary (see Fig. 2).

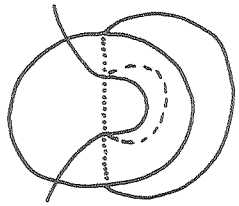

Figure 2

An elementary surface separated into two parts by a non-tree-graph cut.

Non-tree-graph cuts disrupt, therefore, the entropy property that parts are never more complex than the whole, and prevent an orderly topological expansion in which the zero-entropy level is closed in the sense that the discontinuities of zero-entropy functions depend only on zero-entropy functions.

The ordered S-matrix approach leads to rules [3, 4] on the ways two zero-entropy surfaces can be joined together to give contributions to zero-entropy amplitudes. These rules are, however,

not invariant under the operations of crossing and cluster decomposition, and consequently the singularities associated with a given fixed Landau diagram can be classified as zero entropy in some channels but non-zero entropy in other channels. Hence a single singularity surface can belong to different terms in the topological expansion in different channels. An example is shown in Fig. 3.

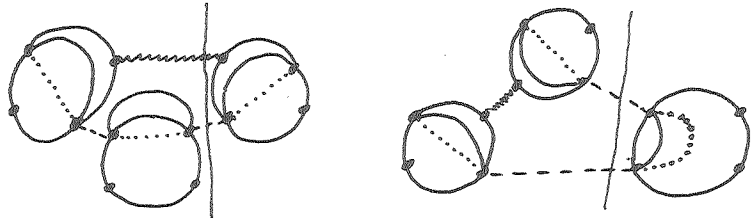

Figure 3

The graphs that represent in different channels the discontinuity around a single triangle-diagram singularity surface.

According to the ordered S-matrix rules the diagram of Fig. 3(a) contributes to the zero-entropy function whereas that of Fig. 3(b) does not. But channel-dependent classifications of this kind lead to unacceptable complications in the analytic structure of the zero-entropy functions, such as the intrusion into their physical sheets of singularities that in the physical functions are buried on unphysical sheets, or are not present at all.

A further difficulty with all these approaches is that zero-entropy amplitudes contain singularities corresponding to non-planar Landau diagrams, and hence presumably have cuts in the complex angular momentum plane.

2. THE ZERO-ENTROPY AMPLITUDES

The difficulties mentioned above can be avoided by treating the three quark lines associated with the baryon unsymmetrically at the zero-entropy level. This allows one to impose at this level a planar structure similar to that obtained in the meson sector, and to represent a typical baryon ortho amplitude by any one of the three equivalent graphs shown in Fig. 4.

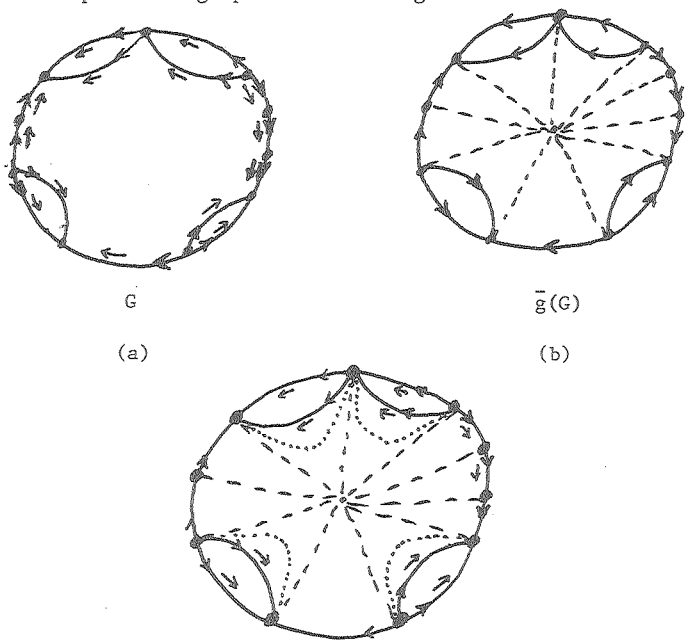

G (a)

$\bar{g}(G)$ (b)

$\hat{g}(G)$ (c)

Figure 4

Three equivalent graphs associated with a typical hadronic amplitude.

Figure 4(a) is the quark graph G. Its edges are directed line segments called quark lines. The small arrow next to each quark-line edge j indicates that the edge should be replaced by the ortho propagator $(p_{aj} \cdot \sigma)/m_{aj}$ in the construction of the zero-entropy amplitude Z^G. For a para case this small arrow would point in the direction opposite to the direction of the quark line, and would indicate that the para propagator $(-p_{bj} \cdot \sigma)/m_{bj}$ should be used.

Figure 4(b) is the particle-quark graph $\bar{g}(G)$. The dashed-line edges of $\bar{g}(G)$ correspond to particles, and the graph $g(G)$ consisting of the dashed-line edges of $\bar{g}(G)$ and the vertices upon which they begin and end is a Landau graph.

A vertex i of G corresponds to a meson, baryon or anti-baryons, or baryonium according to whether two, three, or four quark-line edges are incident upon it. A vertex i with three quark lines terminating on it is called a baryon vertex, and a vertex i with three quark lines originating on it is called an anti-baryon vertex.

Except in the trivial 2-vertex case each vertex of a quark graph G is connected by edges to exactly two other vertices, which are called its neighbors, and at most two edges connect any pair of vertices. If exactly one quark edge connects two vertices then this edge is called a solitary quark line. If exactly two quark edges connect a pair of vertices then these two edges are called paired quark lines.

The diagrams in figures 4(a) and 4(b) are planar graphs. But they can also be considered to represent discs bounded by the peripheral quarks lines. Figure 4(c) is a graph $\hat{g}(G)$ that can be considered to represent a surface that is bounded by all the quark lines, and has three sheets joined together at each dotted (i.e., junction) line. The ortho or para character can then be represented by giving each section of the surface (bounded by quark, particle or junction lines) an orientation that induces on the quark-line boundary a direction that either agrees in the ortho case or disagrees in the para case with the direction of the quark line itself. This surface representation associated with $\hat{g}(G)$ relates the present scheme to the ones proposed earlier. It is used by Chew and Poénaru, who, however, delete from it a small neighborhood of each quark-line vertex. This gives a "feathered" surface analogous to the one bounded by the open diagram D of Fig. 1 of paper I.

The function $Z^G(A)$ associated with G depends on a set of variables A. This set A contains for each vertex i of G a mathematical momentum-energy four-vector p_i. It also contains for each leading end of each quark line j of G a quark variable (α_j, λ_j), and for each trailing end an anti-quark variable $(\dot{\beta}_j, \rho_j)$. The α_j and $\dot{\beta}_j$ are lower undotted and dotted two-valued spinor indices, and λ_j and ρ_j are flavor labels. If the particle associated with vertex i is a Regge recurrence corresponding to orbital angular momentum L_i then this vertex i is associated with a set of $L_i = L$ pairs of indices $(\mu_{i1}, \sigma_{i1}, \mu_{i2}, \sigma_{i2}; \ldots; \xi_{iL}, \sigma_{iL})$,

where μ_{ik} is a vector index associated with orbital angular momentum and σ_{ik} is an associated σ index that will be discussed later.

The function $Z^G(A)$ corresponding to an ortho graph G has the form

$$Z^G(A) = -\pi_j\left(\frac{p_{aj}}{m_{aj}} \cdot \sigma_{\alpha_j\dot{\beta}_j}\, \delta_{\lambda_j\rho_j}\right) f^G(A), \qquad (1)$$

where j runs over the edges of G and $f^G(A)$ is a function of the λ's, ρ's, and σ's, and of the scalar products of the vectors p_i and $e(\mu_{ik})$, which have components p_i^μ and $e(\mu_{ik})^\mu = \delta_{\mu_{ik}}{}^\mu$, respectively. The vector p_{aj} is the vector p_i associated with the vertex i on the leading end of line j. For a para graph G the vector p_{aj} in (1) would be replaced by $(-p_{bj})$, where p_{bj} is the vector p_i associated with the vertex i on the trailing and of line j, and m_{aj} would be replaced by m_{bj}.

To recover from (1) the meson result (3.9), of paper I but with the A of (3.9) now replaced by Z, one contracts, for each meson vertex i, the two spinor indices α_j and $\dot{\beta}_k$ associated with the lines j and k that terminate and originate on vertex i, respectively, against the two associated spinor indices α_j and $\dot{\beta}_k$ of the meson wave function $\psi^{\dot{\beta}_k\alpha_j}(s) = is\cdot\tilde{\sigma}^{\dot{\beta}_k\alpha_j}/\sqrt{2}$ corresponding to that vertex.

The variables in the set of variables A occurring in $Z^G(A)$ are arranged in one of the n standard linear orders corresponding to G. Such an ordering is obtained

by dividing the set of variables A into the disjoint parts A_i associated with the various vertices i of G, and then ordering these parts A_i from right to left according to the order in which the corresponding vertices i of G are encountered by a path that starts just before some vertex of G and runs around the periphery of G, moving always in the direction of all the solitary quark lines and against the directions of all the paired quark lines. The set of variables A_i consists of the ordered set of variables $(p_i;\ \mu_{i1}, \sigma_{i1};\ \cdots\ ;\ \mu_{iL_i}, \sigma_{iL_i})$ followed by an ordered set of spin-flavor variables. These latter variables are the pairs of variables (α_j, λ_j) or $(\dot{\beta}_j, \rho_j)$ associated with the ends of those quarks lines j that terminate or originate on vertex i. They are ordered from right to left in the way in which the associated quark lines j are encountered by the peripheral path if it makes a small inward excursion around vertex i.

The set of quark variables (α_j, λ_j) in A_i, placed in the relative order in which they occur, in A_i, is written

$$(\alpha_{i1}, \lambda_{i1};\ \cdots\ ;\ \alpha_{iN_i}, \lambda_{iN_i}). \qquad (2)$$

The set of anti quark variables $(\dot{\beta}_j, \rho_j)$ in A_i, placed in the relative order in which they occur in A_i, is written

$$(\dot{\beta}_{i\bar{N}_i}, \rho_{i\bar{N}_i};\ \cdots\ ;\ \dot{\beta}_{i1}, \rho_{i1}). \qquad (3)$$

These equations define a labelling convention that will be used later.

By virtue of the ordering conventions established above the ordered set of arguments A_i in $Z^G(A_1, \ldots, A_n) \equiv Z^G(A)$ determines G uniquely apart from the ortho-para specification. The function $Z^{G'(A)} = Z(A)$ is the sum of the functions $Z^G(A)$ overall 2^N possible specifications of the ortho-para characters of the N quark lines of $G'(A)$, which is the graph without the ortho-para arrows.

There are n different standard linear orders of the n variables A_i associated with an n-vertex graph G. These are generated from any one of these orderings by the n cyclic permutations. In accordance with the spin-statistics theorem for physical particles the sign of $Z(A)$ depends on the relative order in which the baryon and antibaryon variables A_i occur in A: a cyclic permutation P of the n variables A_i of A that takes a single variable A_k from one end to the other of the linear sequence converts $Z(A)$ to

$$A(PA) = \pm Z(A),$$

where the sign is plus if A_k is a meson or baryonium variable and minus if it is a baryon or anti baryon variable.

The minus sign appearing in (1) corresponds to any linear ordering of the variables A_i of A that is specified by breaking the cyclic order at a solitary quark line. Breaking at a pair of paired quark lines gives a plus sign.

3. THE ZERO-ENTROPY PART OF M(A)

The physical scattering function $M(A_1, \ldots, A_n) \equiv M(A)$ corresponding to a set of n particles specified by the set of variables $(A_1, \ldots, A_n)$ is the connected part of the S-matrix element specified by these variables, times $[(2\pi)^4 \delta(\Sigma\, p_i)]^{-1}$. The zero-entropy part of $M(A)$ is given by the symmetrized sum of zero-entropy functions:

$$M^Z(A) = \sum_P \sigma(P) Z(PA)/n \qquad (4)$$

The sum is over all permutation operators P of the form

$$P = P_o \prod_{i=1}^{n_i} P_i, \qquad (5)$$

where P_o is any one of the $n!$ permutations of the order of the n variables A_i in A, and P_i is any one of the $\bar{n}_i$ permutations of the order of the quark and anti quark variables in A_i: a permutation P_i can permute the order of the quark variables in A_i and can permute the order of the anti quark variables in A_i, but it never interchanges quark variables with antiquark variables. Thus $\bar{n}_i \equiv \bar{n}(A_i)$ is 1, 6, 6, or 4 for a meson, baryon, anti baryon, or baryonium variable A_i, respectively. The function $Z(PA)$ is defined to be zero unless PA corresponds to some zero-entropy graph G of the kind shown in Fig. 4.

The number $\sigma(P)$ is the signature of the restriction of P_o to baryon and anti baryon variables A_i: it is plus one or minus one according to whether the change produced by P_o in the relative order of the baryon and anti baryon variables A_i in A is generated by an even or odd number of permutations of these variables.

For each permutation P_o there is a set of n permutations that are generated from it by the n cyclic permutations. The $n!$ permutations P_o can be expressed by writing $P_o = P_o'' P_o'$ where P_o'' ranges over the n cyclic permutations and P_o' ranges over a set of $(n-1)!$ permutations P_o not connected by cyclic permutations. The n contributions to (4) arising from a fixed P_o', but with different P_o'', are all equal, and hence one can restrict the sum in (4) to the sum over the $(n-1)!$ permutations P_o', and omit the factor n^{-1}. In this form of (4) there is one contribution from each cyclically ordered set of variables PA that corresponds to a zero-entropy graph of the kind shown in Fig.4: the n different standard linear orders associated with a given graph G do not give separate contributions.

4. PRODUCTS

The discontinuity around any physical-region singularity of any scattering function can be expressed as a linear combination of bubble diagram functions M^B [7, 8]. These functions are represented diagrammatically by bubble diagrams B of the kind shown in Fig. 5.

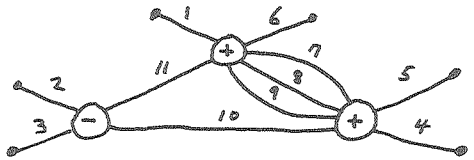

Figure 5

A bubble diagram B.

Each plus bubble b of B is associated with a scattering function $M^b = M_+(A^b)$, where the n_b components A_i^b of A^b correspond one-to-one to the n_b edges of B that are incident upon b. Each minus bubble b of B is associated in the similar way with the function $M^b = M_-(A^b)$, which is the negative of the connected part of the matrix element of $S^\dagger$ specified by A^b, times $[(2\pi)^4 \delta(\Sigma p_i)]^{-1}$. The plus-minus sign in $M_\pm(A^b)$ is often considered part of A^b. Then $M^b = M(A^b)$.

In general, a bubble diagram B is a Landau graph $g(B)$ with each internal vertex replaced by a plus or minus bubble. Each edge

j of a Landau graph $g(B)$, or bubble diagram B, is associated with a particle-type label $t_j^{g(B)} \equiv t_j^B$. This type variable t_j^B is a partial characterization of A_j^B: it can place restrictions on p_j^2, on the (unordered set of) flavor variables, on the orbital variables μ_{jk} and σ_{jk}, and on the quark versus antiquark character of each spin-flavor label.

Each internal edge j of B connects a bubble $b'(j)$ of B to another bubble $b''(j)$, and defines a pairing of a component $A_{i'(j)}$ of $A^{b'(j)}$ with a component $A_{i''(j)}$ of $A^{b''(j)}$. For notational convenience the indices i are arranged so that $i'(j) = j$, where $p^o_{i'(j)} = p^o_j$ is positive.

The bubble diagram function M^B corresponding to bubble diagram B is

$$M^B = \sigma^B \oint \left(\prod_{b\in B} M^b\right) H^B(n^B)^{-1}\, \omega^{g(B)} . \tag{6}$$

The factor $\omega^{g(B)}$ is the integrand of the integral that defines the phase-space factor $f^{g(B)}$ corresponding to the graph $g(B)$:

$$\omega^{g(B)} = \prod_j \left((2\pi)\delta(p_j^2 - m_j^2)\ \theta(p_j^o)\ d^4p_j(2\pi)^{-4}\right)$$

$$\times \prod_b{}' \left((2\pi)^4 \delta\left(\Sigma \varepsilon^{g(B)}_{bj} p_j\right)\right) . \tag{7}$$

Here j runs over the set of internal edges of $g(B)$, and b

runs over all but any one of the set of internal vertices of $g(B)$. The matrix elements ε^g_{bj} are matrix elements of the incidence matrix associated with graph g.

The function H^B has the form $H^B = \prod_j h_j^B/\bar{n}_j$ where j runs over the internal edges of B, and

$$h_j^B = \theta_j^B \prod_{k=1}^{L_j} (-g^{\mu_{i''(j)k}\mu_{jk}})\delta_{\sigma_{i''(j)k}\sigma_{jk}}$$

$$\prod_{k=1}^{N_j} v_j \cdot \tilde{\sigma}^{\dot{\beta}_{i''(j)k}\alpha_{jk}}\ \delta_{\rho_{i''(j)k}\lambda_{jk}}$$

$$\prod_{k=1}^{\bar{N}_j} v_j \cdot \tilde{\sigma}^{\dot{\beta}_{jk}\alpha_{i''(j)k}}\ \delta_{\rho_{jk}\lambda_{i''(j)k}} \tag{8}$$

The function θ_j^B is unity if $L_j = L_{i''(j)}$, $N_j = \bar{N}_{i''(j)}$, $\bar{N}_j = N_{i''(j)}$, $p_j = -p_{i''(j)}$, and A_j^B conforms to the partial restrictions imposed by the type variable t_j^B. Otherwise θ_j^B is zero. The remaining symbols in (8) are defined in (2), or as in (2.18) of I, or by Kroenecker.

The summation sign in (6) signifies a summation over the discrete indices occurring in H^B. For each of the upper spinor or vector spinor indices of H^B there is, according to (2), an equal lower spinor or vector index in one of the functions M^b. Hence these sums constitute covariant contractions. Each flavor- and σ-index of H^B also is contracted with an identical flavor- or σ-index in one of the M^b.

To fixed the sign σ^B in (6) the diagram B is drawn on a plane with no edges crossing through bubbles, and with the external edges of B extended out to a big circle that encloses B. The variables A_i^b or A_i^B occurring in the arguments of the individual functions $M(A^b)$ or in the arguments of the bubble diagram function M^B itself are ordered from right to left according to the sequence in which the associated vertices i are encountered by a path that starts at the top of the bubble or big circle and proceeds clockwise. The sign σ^B is then a product of factors (- 1), one for each crossing of a pair of fermion edges in this diagrammatic representation of B.

The factor n^B in (6) is the symmetry number of the bubble diagram B: it is the number of distinct permutations π: (b, j) → (πb, πj) on the bubbles b and <u>internal</u> edges j of B that leave B unchanged in the sense that if $\varepsilon_{b,j}^{g(B)} = \varepsilon_{b,j}^B$ are the elements of the incidence matrix of the graph g(B), and σ_b^B is the sign of bubble b of B, then the following invariance conditions hold:

$$\varepsilon_{\pi b,\pi j}^B = \varepsilon_{b,j}^B \qquad \text{(all b and j)}, \tag{9.a}$$

$$\sigma_{\pi b}^B = \sigma_b^B \qquad \text{(all b)}, \tag{9.b}$$

and

$$t_{\pi j}^B = t_j^B \qquad \text{(all j)}. \tag{9.c}$$

Two bubble diagrams B' and B'' are topologically equivalent if and only if there is a permutation π of the bubbles b and internal edges j of B' such that

$$\varepsilon_{\pi b,\,\pi j}^{B'} = \varepsilon_{b,j}^{B''} \qquad \text{(all b and j)}, \tag{10.a}$$

$$\sigma_{\pi b}^{B'} = \sigma_b^{B''} \qquad \text{(all b)}, \tag{10.b}$$

and

$$t_{\pi j}^{B'} = t_j^{B''} \qquad \text{(all j)}. \tag{10.c}$$

The discontinuity formulas [7, 8, 9] specify that there is only one contribution from each set of topologically equivalent bubble diagrams: two topologically equivalent bubble diagrams B' and B'' do not give additive contributions $M^{B'}$ and $M^{B''}$ to the discontinuity.

The sign σ^B was fixed by drawing B with the edges j incident upon each bubble b ordered in some definite way. A change in these orders gives a topologically equivalent diagram B that gives no additional contribution to the discontinuity.

A <u>fully labelled</u> bubble diagram $\bar{B}$ compatible with a bubble diagram B is a diagram that can be constructed by assigning to the end $i'(j)$ of each internal edge j of B a set of variables $A_{i'(j)}^{\bar{B}}$, assigning to the end $i''(j)$ of each internal edge j of B a set of variables $A_{i''(j)}^{\bar{B}}$, where $A_{i'(j)}^{\bar{B}}$ and $A_{i''(j)}^{\bar{B}}$ must be such that $\theta_j^B \neq 0$, and assigning a set of variables A_e^B

to both ends of each external edge e of B. Two fully labelled bubble diagrams $\bar{B}'$ and $\bar{B}''$ are topologically equivalent if and only if there is a permutation π of the bubbles b and internal edges j of $\bar{B}'$ such that

$$\epsilon^{\bar{B}'}_{\pi b,\pi j} = \epsilon^{\bar{B}''}_{b,j} \qquad \text{(all } b \text{ and } j\text{)}, \tag{11.a}$$

$$\sigma^{\bar{B}'}_{\pi b} = \sigma^{\bar{B}''}_{b} \qquad \text{(all } b\text{)}, \tag{11.b}$$

$$A^{\bar{B}'}_{i''(\pi j)} = A^{\bar{B}''}_{i''(j)} \qquad \text{(all } j\text{)}, \tag{11.c}$$

and

$$A^{\bar{B}'}_{i'(\pi j)} = A^{\bar{B}''}_{i'(j)} \qquad \text{(all } j\text{)}. \tag{11.d}$$

The sums and integrals that occur in the definition (6) of M^B can be regarded as a summation over the fully labelled $\bar{B}$ compatible with B. If the variables p_j associated with the lines j of $\bar{B}$ are all different, as they are on all but a set of zero measure, then M^B contains the contributions from n^B topologically equivalent fully labelled diagrams $\bar{B}$. These n^B contributions are all equal. Thus the factor $(n^B)^{-1}$ in (6) can be replaced by a factor $\theta^{\bar{B}}$ that takes on values zero or one (except on sets of zero measure) in such a way as to allow a non zero contribution from only one of any set of topologically equivalent $\bar{B}$. On the sets of zero measure $\theta^{\bar{B}}$ is the inverse of the number of permutations π that leave $\bar{B}$ unchanged. Thus, apart

from this minor complication on sets of zero measure, the contribution to the discontinuity associated with B is simply a sum over any complete set of topologically inequivalent fully labelled bubble diagrams $\bar{B}$ compatible with B:

$$M^B = \sigma^B \sum_{\bar{B}\subset B} \prod_b M^{b(\bar{B})} \prod_j \left(\bar{h}_j/\bar{n}_j\right) \theta^{\bar{B}} \omega^{\bar{B}}, \tag{6'}$$

where the bubble diagram B is considered here to be a symbolic representation for the set of $\bar{B}$ compatible with B, and a sum-integral over $\bar{B}$ is a sum over the discrete variables associated with the internal edges j of the labelled diagram $\bar{B}$ and an integral over the momentum-energy variables $p_j = p_{i'(j)} = -p_{i''(j)}$ associated with the internal edges j of $\bar{B}$. The factor $\omega^{\bar{B}}$ is the factor represented by $\omega^{g(B)}$ in (6) and (7).

The above discussion specifies the sign and symmetry factors connected with the usual bubble diagram functions M^B. Let Z^B denote the part of M^B that arises from the zero-entropy parts of the functions M^b associated with the bubbles b of B. The function Z^B is obtained by replacing each factor $M^b = M(A^b)$ in M^B by its zero-entropy part $M^Z(A^b)$ defined in (4).

The sum in (4) over the permutations P includes a sum over the $\bar{n}_j$ permutations $P_i = P_{i'(j)} = P_j$ in (5). This latter sum converts the P_i in P in (4) to a factor

$$\sum_{k=1}^{\bar{n}_j} P_{jk} \,. \tag{12.a}$$

This factor stands on one side of the metric matrix h_j^B in (8). On the other side stands a similar factor

$$\sum_{k=1}^{n_j} P_{i''(j)k}, \qquad (12.b)$$

which can be commuted through h_j^B and combined with the factor (12.a) to give just $\bar{n}_j$ times this factor (12.a). The extra numerical factor $\bar{n}_j$ cancels against the factor $\bar{n}_j^{-1}$ that occurs in (6') to give for the net result precisely the factor (12.a), which stands together with h_j^B between the two zero-entropy functions. Thus, for example, the baryon connection represented by the top-left diagram in Fig. 6 can be replaced by the sum of the quark connections represented by the rest of Fig. 6, provided each line segment on the right-hand side of the second equation in Fig. 6 is considered to represent now the product of a flavor delta function and a spin metric-factor $v \cdot \tilde{\sigma}$.

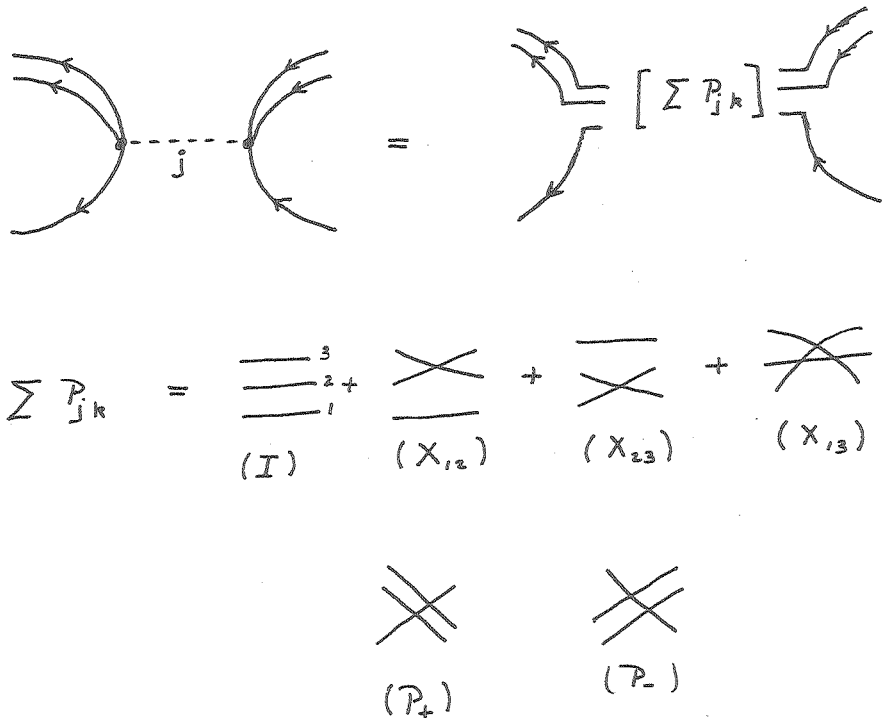

Figure 6

Diagrammatic representation of the sum of quark-edge connections entailed by a baryon connection j. The factor ΣP_{jk} stands together with h_j^B between the two zero-entropy functions.

The baryon connection J thus gives a sum over the 3! ways of joining the three quark lines that come into vertex i'(j) [or i"(j)] to the three quark lines that leave vertex i"(j)[or i'(j)]. Of course, some or all of these 3! terms may give a null contribution, due, for example, to a mismatching of the flavors of the two quarks on the two ends of one or more of the connecting quark segments in Fig. 6: the Kroenecker delta functions $\delta_{\lambda\rho}$ in h_j^B cause the vanishing of a contribution in which any two such flavors differ.

It should be noted that our normalization of $M(A^b)$ corresponds to a normalization of the corresponding S matrix $S(A^b)$ that leaves out the traditional factor $(n_j)^{-1/2}$ associated with n_j identical quarks (or anti quark) in particle j. This factor is absorbed instead into the normalization factor $\bar{n}_j$ appearing in H^B. Then the identical-quark case can be treated together with the nonidentical-quark case, without special consideration.

Consider now a contribution to Z^B corresponding to some $\bar{B}$ in which all the labels p_j are different. The set of edges incident upon any bubble b of $\bar{B}$ can be arranged in some definite order and there will be (in the θ form (6') or M^B) a nonzero contribution from only this one way of connecting the particle edges j to the bubbles b of B. However, the sum in (4) over the $(n_b - 1)!$ permutations P'_o associated with bubble b gives a term $Z(PA^b)$ for each of the $(n_b - 1)!$ different cyclic orders of the set of variables A_i^b. Some of these orders may give a null contribution, because only certain orderings of variables correspond to allowed zero-entropy graphs (See Fig. 4). Thus the sum generated by the permutations P'_o associated with the fixed bubble b can be restricted to a sum over those different cyclic orderings of the variables A_i^b that correspond to a zero-entropy graph $G(PA^b)$. For each bubble b of B

there is a sum of this kind. Thus the contribution to M^B from terms corresponding to the fixed $\bar{B}$ is just a sum over terms corresponding to any complete set of topologically ineqivalent quark graphs $\bar{g}$ compatible with B. And the full function Z^B is a sum-integral over any complete set of topologically inequivalent fully labelled particle-guark graphs $\bar{g}$ compatible with B. The concepts just introduced are now defined.

A particle-quark graph $\bar{g}$ compatible with B is a graph $\bar{g}$ that can be formed by replacing each bubble b of B by a quark graph $G^b(\bar{g})$, with each edge of B that is incident upon b connected in $\bar{g}$ to a different vertex i of $G^b(\bar{g})$. (See Fig.7) The number of quark lines originating and terminating on this vertex i of $G^b(\bar{g})$ must accord with the type t_j^B or t_e^B of edge j or e of B. This is illustrated in the top-left diagram of Fig. 6, for the case of a baryon edge j.

A <u>fully labelled</u> graph $\bar{g}$ compatible with B is a particle-quark graph compatible with B that has a label $A_i^{\bar{g}}$ attached to each quark vertex i, with the labels $A_{i'(j)}^{\bar{g}}$ and $A_{i''(j)}^{\bar{g}}$ restricted by the condition that $\theta_j^B \neq 0$. Two such fully labelled graphs $\bar{g}'$ and $\bar{g}''$ are topologically equivalent if and only if there is a permutation $\pi:(i, j, k) \to (\pi i, \pi j, \pi k)$ of the internal vertices i of $\bar{g}'$, the internal particle edges j of $\bar{g}'$, and the quark lines k of $\bar{g}'$ such that

$$\varepsilon^{\bar{g}'}_{\pi i,\pi j} = \varepsilon^{\bar{g}''}_{i,j} \qquad \text{(all i and j)}, \tag{13.a}$$

$$\varepsilon^{\bar{g}'}_{\pi i,\pi k} = \varepsilon^{\bar{g}''}_{i,k} \qquad \text{(all i and k)}, \tag{13.b}$$

$$\sigma^{\bar{g}'}_{\pi i} = \sigma^{\bar{g}''}_{i} \qquad (13.c)$$

and

$$A^{\bar{g}'}_{\pi i} = A^{\bar{g}''}_{i} \quad \text{(all } i\text{)}. \qquad (13.d)$$

Here $\sigma^{\bar{g}}_{i}$ is the sign of the bubble in which vertex i lies.

The result stated above combined with that expressed by Fig. 6 entails that

$$Z^B = \sigma^B \sum_{\bar{g}\subset B} H^{\bar{g}} \prod_b Z^{G^b(\bar{g})} \quad \theta^{\bar{g}} \omega^{\bar{g}} \qquad (14)$$

where the sum-integral is over all fully labelled graphs $\bar{g}$ compatible with B: it is a sum over the different (unlabelled) graphs $\bar{g}$ compatible with B, a sum over the discrete indices of $A_{i'(j)}$ and $A_{i''(j)}$ associated with the internal particle edges j of $\bar{g}$, and an integral over the momentum-energy vectors $p_j = p_{i'(j)} = -p_{i''(j)}$ associated with the internal particle edges j of $\bar{g}$. The function $\theta^{\bar{g}}$ is zero or one (except on a set of zero measure) in such a way as to allow precisely one contribution from any set of fully-labelled graphs $\bar{g}$ that are topologically equivalent. The factor $\theta^{\bar{g}}$ can be replaced by the inverse of $n^{\bar{g}}$, which is the number of permutations $\pi(i, j, k) \to (\pi i, \pi j, \pi k)$ that satisfy (13) with $\bar{g}'$ and $\bar{g}''$ replaced by $\bar{g}$. This latter form correctly weights the sets where two p_j's coincide. Normally $\theta^{\bar{g}} = n^{\bar{g}} = 1$: these factors are included as an extra precaution against over counting, and to maintain the similarity to earlier formulas.

The factor $H^{\bar{g}}$ in (14) is

$$H^{\bar{g}} = \prod_j \left(h_j \sum_{k=1}^{n_j} P_{jk} \right) \prod_e \left(\sum_{k=1}^{n_e} P_{ek} \right) \quad , \qquad (15)$$

where j and e run over the internal and external particle edges of $\bar{g}$, respectively. The factors P_{jk} and P_{ek} in (15) are operators whose action is now described.

The set of variables A_j include the set $a_j = (a_{j1}, \ldots, a_{jN_j})$ of spin-flavor indices, the set $\sigma_j = (\sigma_{j1}, \ldots, \sigma_{jL_j})$ of σ indices, and the set $\mu_j = (\mu_{j1}, \ldots \mu_{jL_j})$ of orbital indices. The permutation $P_{jk} = P$ is specified by a permutation $P: (1, \ldots, N_j) \to (P1, .., PN_j)$ of the set of N_j integers. For example, if $P_{jk} = P$ is the permutation P_- represented by the last diagram of Fig. 6 then (P1, P2, P3) = (3, 1, 2). If j is a baryon edge then each index σ_{jk} is two-valued and these two values together with a sequence (P1, .., P3) designate two orthonormal vectors

$$|\sigma, (P1, P2, P3)) = \begin{cases} \dfrac{|p1\rangle - |P3\rangle}{\sqrt{2}} & (\sigma = 1) \\ \dfrac{2\,|P2\rangle - |P1\rangle - |P3\rangle}{\sqrt{6}} & (\sigma = 2) \end{cases} , \qquad (16)$$

where $\langle n|m\rangle = \delta_{nm}$ for any integers n and m. If j is a

baryonium edge then each index σ_{jk} is three-valued, and for each permutation (P1, P2, P3, P4) of the four integers (1, 2, 3, 4) an orthonormal set of three vectors is defined:

$$|\sigma, (P1, P2, P3, P4)) = \begin{cases} \dfrac{|P1> - |P2>}{\sqrt{2}} & (\sigma = 1) \\ (|P1> + |P2> & \\ - |P3> - |P4>)/2 & (\sigma = 2) \\ \dfrac{|P3> - |P4>}{\sqrt{2}} & (\sigma = 3) \end{cases} \tag{17}$$

The permutation operator $P_{jk} = P$ acts in the space associated with the variables (a_j, σ_j), and has matrix elements

$$\begin{aligned} &P(a_j, \sigma_j; a_j', \sigma_j') \\ &= \prod_{i=1}^{N_j} <a_{j,Pi} | a_{ji}'> \\ &\times \prod_{i=1}^{L_j} <\sigma_{ji}, (1, \ldots, N_j) | \sigma_{ji}', (P1, \ldots, PN_j)>, \end{aligned} \tag{18}$$

where $<a|a'> = \delta_{aa'}$. The operator P_{jk} in (14) acts on $M^{b'(j)}(A_j)$ as follows:

$$\begin{aligned} &P_{jk} M^{b'(j)}(p_j, a_j, \sigma_j, \mu_j) \\ &= P_{jk}(a_j, \sigma_j; a_j', \sigma_j') M^{b'(j)}(p_j, a_j', \sigma_j', \mu_j) \end{aligned} \tag{19}$$

where a sum over the repeated indices a_j' and σ_j' is implied.

The operators P_{ek} are defined analogously.

This concludes the description of the sign, symmetry, and statistical factors in the bubble diagram functions M^B, and in the parts Z^B of these functions that arise from the zero-entropy contributions to the scattering functions M^b corresponding to their bubbles b.

5. PARTICLE VARIABLES

The sum of permutation operators P_{jk} occurring in (15) can be written

$$\sum_{k=1}^{n_j} P_{jk} = n_j \hat{P}_j, \tag{20}$$

where $\hat{P}_j$ is a projection operator onto a symmetrized subspace of the space spanned by the vectors $|a_j, \sigma_j>$. The projection operator $\hat{P}_j$ can be written in the form

$$\hat{P}_j = \sum_{\hat{a}_j} |\hat{a}_j><\hat{a}_j|, \tag{21}$$

where $\hat{a}_j$ is a set of indices that labels the vectors of an orthonormal basis of the symmetrized subspace.

The part of the integrand of (14) that is associated with edge j of B is

$$Z^{G^{b''(j)}(\bar{g})} \left(A^{b''(j)}(\bar{g})\right)_{h_j} \Sigma P_{jk}$$

$$Z^{G^{b'(j)}(\bar{g})} \left(A^{b'(j)}(\bar{g})\right)$$

$$\equiv <Z_j'' |a_j', \sigma_j'> <a_j', \sigma_j'|h_j|a_j, \sigma_j>$$

$$<a_j, \sigma_j|\Sigma P_{jk}|Z_j'>$$

(Eq. 22 continued on next page)

(Eq. 22 continued)

$$= <Z_j''|h_j n_j \hat{P}_j|Z_j'>$$

$$= \sqrt{n_j} <Z_j''|h_j \hat{P}_j|Z_j'> \sqrt{n_j}$$

$$= \sqrt{n_j} <Z_j''|\hat{P}_j h_j \hat{P}_j|Z_j> \sqrt{n_j}$$

$$= \sqrt{n_j} <Z_j''|\hat{a}_j><\hat{a}_j|h_j|\hat{a}_j><\hat{a}_j|Z_j'> \sqrt{n_j} \tag{22}$$

The result of applying this transformation of variables to each edge j and e takes (14) to the form

$$\hat{Z}^B = \sigma^B \sum_{\bar{g}CB} \prod_b \left(\hat{Z}^{G^b(\bar{g})}\right) \hat{H}^{\bar{g}} \hat{\theta}^{\bar{g}} \omega^{\bar{g}}, \tag{23}$$

where the carets on $\hat{Z}$, $\hat{H}$ and $\hat{\sigma}$ indicate that the variables (a_j, σ_j) are replaced by the variables $\hat{a}_j$. Moreover, a factor $\sqrt{n_j}$ for each edge j of B incident upon b has been introduced into $\hat{Z}^{G^b(\bar{g})}$.

The orbital quantum numbers in $\hat{A}_j = (p_j, \mu_j, \hat{a}_j)$ are separate from the spin quantum numbers that occur in $\hat{a}_j$. Rest-frame Clebsch-Gordon combinations gives states of definite J, which are precisely the particle states of the constituent quark model [10]. Boosts from the rest frame give covariant forms of the $h_j^{\bar{g}}$ for states of fixed J. Use of these variables gives an alternative

form of (23):

$$\tilde{Z}^B = \sigma^B \sum_{\bar{g}CB} \prod_b \tilde{Z}^{G^b(\bar{g})} \tilde{H}^{\bar{g}} \tilde{\sigma}^{\bar{g}} \omega^{\bar{g}} , \qquad (24)$$

where the tilde over $\tilde{Z}$, $\tilde{H}^B$, and $\tilde{\sigma}^{\bar{g}}$ signifies the use of the variables $\tilde{A}_j$ of the constituent quark model.

The functions $\tilde{Z}^{G^b(\bar{g})}$ depend on the quark diagram $G^b(\bar{g})$, and hence on the order of the variables, $\tilde{A}^b_i$ in $\tilde{A}^b$. But, in contrast to the case of the zero-entropy functions $Z^{G^b(\bar{g})}$, the individual variables $\tilde{A}^b_i$ occurring in the argument of $\tilde{Z}^{G^b(\bar{g})}$ do not specify, for example, which of the three flavors is to be assigned to the solitary quark edge incident upon a baryon vertex i of $\bar{g}$.

In principle the intermediate particles occurring in (24) include only the stable particles, but important cut contributions can often be simulated by contributions from poles lying close to the physical region.

6. TOPOLOGICAL EXPANSION A

By virtue of the cyclic ordering of the variables associated with any zero-entropy function $Z^{G^b(\bar{g})}$, $\hat{Z}^{G^b(\bar{g})}$, or $\tilde{Z}^{G^b(\bar{g})}$, a topological expansion essentially identical to that of paper I can be introduced. This expansion is defined by specifying that the zero-entropy quark graphs $G^b(\bar{g})$ be placed on an oriented surface Σ with the directions of all solitary quark lines agreeing with the direction induced by the orientation of Σ, and with the directions of all paired quark lines opposing the direction induced by the orientation of Σ. The orientation of Σ as represented on paper is taken to be clockwise. (See Fig. 7)

All quark-particle graphs $\bar{g}$ formed by connecting zero-entropy graphs G by particle lines in the manner discussed in the proceeding section are then classified by their boundary structure and topological index $\lambda(\bar{g})$.

The boundary structure is specified by a decomposition of the external particle edges into a set of cyclic sets corresponding to the set of boundaries of $\bar{g}$. The topological index is given by

$$\lambda(\bar{g}) = e(\bar{g}) - v(\bar{g}) - \omega(\bar{g}) + 1 \qquad (25.a)$$

where e, v, and ω stand for numbers of edges, vertices and windows, of the graph, or equivalently by

$$\lambda\left(g(\bar{g})\right) = e\left(g(\bar{g})\right) - v\left(g(\bar{g})\right) - \omega\left(g(\bar{g})\right) + 1 \qquad (25.b)$$

where $g(\bar{g})$ is the Landau graph obtained by contracting to point vertices the quark graphs $G^b(\bar{g})$ but retaining the cyclic order in which the edges are incident upon these vertices. The boundary structure and topological index together is denoted by $\tau(\bar{g})$.

The topological expansion asserts that M can be decomposed into a sum of terms M^τ corresponding to different topological types τ, and that when any equation $X = 0$ derived solely from unitarity and cluster decomposition is separated into parts of different topological character then each such part of the equation is separately satisfied:

$$X = \Sigma X^\tau = 0 \quad \text{implies} \quad X^\tau = 0 \quad (\text{all } \tau). \tag{26}$$

No cancellations among the parts X^τ of different topological type τ are required.

The "ordered amplitudes" are the parts M^τ corresponding to $\lambda = 0$ and a single boundary. The constituent-quark model particle. The variables $\tilde{A}_i$ can be used. The ordered amplitudes satisfy the closed, planar discontinuity formulas: their discontinuity formulas are the same as those of the physical scattering functions except that the contribution M^B associated with bubble diagram B is reduced to a sum of terms corresponding to the different ways the Landau graph $g(B)$ can be drawn as a planar graph $g_p(B)$, and for each such term the scattering function M^b associated with bubble b of B is replaced by the ordered amplitude

specified by the cyclic order in which the lines of $g_p(B)$ enter vertex b.

Summation of the ordered amplitudes associated with any process gives the planar amplitude, which is the first approximation to the physical scattering function. The situation is essentially identical to that described by Chew and Rosenzweig [11].

Pure baryonium states do not couple to pure meson states at the planar level, and hence the planar baryonium Regge trajectories are distinct from the planar meson trajectories. The selection rule forbidding baryonium-meson transitions arises from the fact that in the particle graphs $g(\bar{g})$ the mesons edges connect only to each other and to the left-hand sides of the (directed) baryon lines, whereas baryonium edges connect only to each other and to the right-hand sides of baryon lines.

As in the meson sector the ordered amplitudes M^τ are not equal to the zero-entropy functions $\tilde{Z}^{G^b}$. In the meson sector the ortho-para transitions were considered elements of complexity, and the zero-entropy amplitudes corresponded to the planar graphs $\bar{g}$ having no such transitions. In the general hadron case there is an added element of complexity associated with the crossings of quark lines illustrated by the last five terms in Fig. 6. Thus in the general case the zero-entropy amplitudes correspond to the graphs $(\bar{g}$ or $g(\bar{g}))$ having one boundary, topological index zero, no ortho-para transitions, and no quark-line crossings.

The zero-entropy level is also a closed, planar level: the discontinuity formulas for the zero-entropy functions are identical

to those for the physical scattering functions except that the discontinuities associated with non-planar Landau graphs are zero and the discontinuity formulas associated with planar Landau graphs have, throughout, zero-entropy amplitudes in place of physical scattering amplitudes. The spin factors factor out.

In specifying the ordered level of the topological expansion, and all higher-order levels, the topological character of a contribution is completely characterized by the boundary structure and topological index λ of the associated graph $\bar{g}$, or $g(\bar{g})$. For specifying the zero-entropy level one must assign an ortho or para character ϵ_b to each guark line of $\bar{g}$, and a permutation P_{jk} to each internal particle edge j of $\bar{g}$, or $g(\bar{g})$. This latter permutation is represented diagrammatically by "thickening" the particle edge into a ribbon lying on Σ, and drawing on this ribbon the appropriate permutation, as illustrated in Fig. 6.

The zero-entropy amplitudes are distinguished from the ordered amplitudes in several ways. Each "particle" j at the zero-entropy level is identified by a set of variables A_j in which the linear order of the spin-flavor variables is fixed. At the ordered level each basic particle is specified by a set of variables that specifies a particle of the constituent quark model, and these latter particles are invariant under permutations of the quarks [and likewise the anti quarks] in the particle. On the other hand, the portion of any boundary or orbit lying between two vertices has a single well-defined flavor for any graph $\bar{g}$

corresponding to a zero-entropy amplitude, whereas for graphs $\bar{g}$ corresponding to ordered amplitudes flavor is not necessarily conserved on the boundary in this way.

7. TOPOLOGICAL EXPANSION B

The topological classification scheme described in the preceding section involves placing the quark graphs G on surfaces that are everywhere locally topologically equivalent to parts of a plane. Another possibility is to place the particle-quark graphs $\hat{g}(G)$ of the kind shown in Fig. 4, and also the graphs constructed from them by product-composition, on "feathered" surfaces, which are surfaces containing junction lines at which three planar surfaces, called feathers, are joined.

Consider two particle-quark graphs $\hat{g}(G_1)$ and $\hat{g}(G_2)$ and the corresponding feathered surfaces $\Sigma(g_1)$ and $\Sigma(g_2)$ upon which they lie. The surface $\Sigma(G_i)$ is bounded by the quark lines of $\hat{g}(G_i)$, and it contains in its interior the particle and junction lines of $\hat{g}(G_i)$. Let these two graphs have two peripheral vertices V_1 and V_2, respectively, that are joined by a particle-connection line. This particle-connection line corresponds to a sum of possible quark line permutations, as indicated in Fig. 6.

Consider the direct connection denoted in Fig. 6 by I. It generates a natural connection of $\Sigma(G_1)$ to $\Sigma(G_2)$. This connection is constructed by removing a small part of $\Sigma(G_1)$ around V_1 and a small part of $\Sigma(G_2)$ around V_2, and then fusing the remaining parts of the two surfaces together in the natural way.

Consider next a term in the particle connection corresponding to a two-quark exchange of the kind denoted in Fig. 6 by X_{ij}. It is represented by including in the surface Σ a twisted strip that forms a bridge between the outer boundaries of the affected feathers. This

bridge effects the required quark exchange.

Consider, finally, a term in the particle connection corresponding to a cyclic permutation of the kind represented in Fig. 6 by P_+ or P_-. It is represented by including in Σ a triangular bridge between the outer boundaries of the three affected feathers. Each side of the triangle is identified with a portion of the outer boundary of one feather, in such a way as to effect the required cyclic permulation of the quark lines.

This way of representing the permulations by connections on the feathered surface was suggested by J. Finkelstein, and has been adopted by Chew and Poénaru. The considerations of the earlier sections apply equally to schemes A and B, since the set of quark graphs is the same in the two schemes, as are the subsets corresponding to the zero entropy, ordered, and planar levels of the topological expansion. Thus the analysis of earlier sections, though originating from a graphical formulation of the baryon topological expansion, provides the analytic foundation also for the recent applications[12,13] formulated within the richer surface-based topological framework developed by Chew and Poénaru.

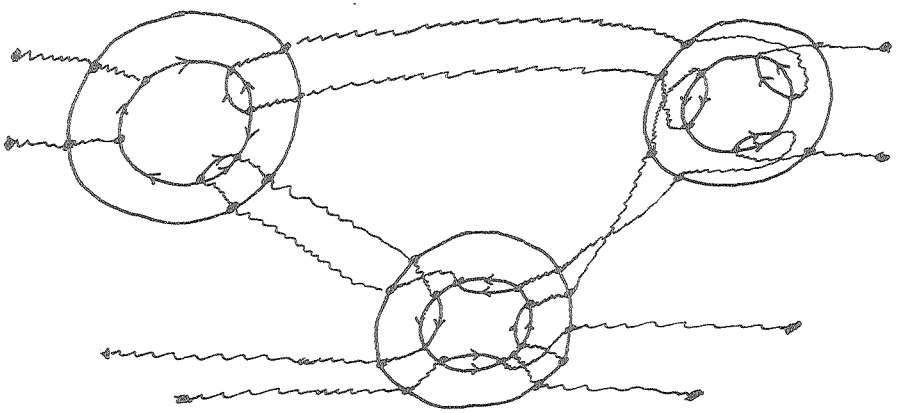

Figure 7. A particle-quark graph $\bar{g}$ representing a typical contribution to Z^B. The three outer circles represent the bubbles b of B. Each encloses a graph that represents a contribution $Z(PA^b)$ to $M^Z(A^b)$.

ACKNOWLEDGEMENT

Much of the stimulation for this work originated in conversations with Geoffery Chew. This work was supported by the Director, Office of Energy Research, Office of High Energy and Nuclear Physics, Division of High Energy Physics of the U.S. Department of Energy under Contract W-7405-ENG-48.

REFERENCES

[1] H. P. Stapp, Lett. Nuovo Cim. 19 (1977) 622
F. J. Capra, Phys. Lett. 68B (1977) 93

[2] G. G. Rossi and G. Veneziano, Nucl. Phys. B123 (1976) 507

[3] K. Konishi, Nucl. Phys. B131 (1977) 143

[4] G. F. Chew, J. Finkelstein, J. P. Sursock, and G. Weissmann, Nucl. Phys. B136 (1978) 493

[5] J. P. Sursock, General Topological Expansion of Hadrons Amplitudes, Lawrence Berkeley Laboratory Report LBL-7588 (1978)

[6] H. P. Stapp, Nuovo Cim. 46A (1978) 37

[7] J. Coster and H. P. Stapp, J. Math. Phys. 10 (1969) 371
J. Math. Phys. 11 (1970), 1441, 2743
and in Structural Analysis of Collision Amplitudes, ed. R. Barlian and D. Iagolnitzer (North-Holland, New York, 1976) 195

[8] R. J. Eden, P. V. Landshoff, D. I. Olive, J. C. Polkinghorne, The Analytic S-matrix (Cambridge Univ. Press, 1966) 238

[9] J. Coster and H. P. Stapp, J. Math. Phys. 10 (1969) App. A.

[10] N. Isgur and G. Karl, Phys. Rev. D18 (1978) 4187, D19 (1979) 2653

[11] G. F. Chew and C. Rosensweig, Physics Reports 41C (1978) 263

[12] G. F. Chew, Phys. Rev. Lett. 47 764-767 1981.

[13] G. F. Chew, J. Finkelstein, and M. Levinson, Phys. Rev. Lett. 47, 767-770.

FIGURE CAPTIONS

Figure 1. Three Elementary surfaces.

Figure 2. An elementary surface separated into two parts by a non-tree-graph cut.

Figure 3. The graphs that represent in different channels the discontinuity around a single triangle-diagram singularity surface.

Figure 4. Three equivalent graphs associated with a typical hadronic amplitude.

Figure 5. A bubble diagram B.

Figure 6. Diagrammatic representation of the sum of quark-edge connections entailed by a baryon connection j. The factor ΣP_{jk} stands together with h_j^B between the two zero-entropy functions.

Figure 7. A particle-quark graph $\bar{g}$ representing a typical contribution to Z^B. The three outer circles represent the bubbles b of B. Each encloses a graph that represents a contribution $Z(PA^b)$ to $M^Z(A^b)$.